Jae-Jun Kim
NRC Research Associate
e-mail: jkil@nps.edu
Naval Postgraduate School, Department of Mechanical and Astronautical Engineering, Monterey, CA 93943

Tarunraj Singh
Professor
e-mail: tsingh@eng.buffalo.edu
Department of Mechanical & Aerospace Engineering, State University of New York at Buffalo, Buffalo, NY 14260

Controller Design for Flexible Systems With Friction: Pulse Amplitude Control

Accounting for friction is important when designing controllers for precision motion control systems. However, the presence of the friction and the flexibility in the system yields undesirable behaviors such as residual vibration and stick-slip oscillation near the reference value. In the proposed development, a pulse amplitude modulated controller with user-specified pulse width, is used to initiate the motion so as to permit the system to coast to the desired final position after the final pulse, with zero residual vibrations. The proposed technique is illustrated on the floating oscillator benchmark problem, where friction acts on the first mass. Numerical simulation illustrates the effectiveness of the proposed technique. [DOI: 10.1115/1.1988341]

1 Introduction

Friction is highly nonlinear in the low-velocity region and when there is a velocity reversal. For precise positioning and pointing systems, difficulty in control arises near the desired final position because of stiction. Conventional PD and PID controllers are known to cause steady-state error and hunting [1]. Yang and Tomizuka [2] developed the adaptive pulse width control technique for rigid body systems. The pulse width control can avoid the problems of hunting and velocity reversals by allowing the system to coast toward the desired position. To account for imperfect knowledge of the system parameters which result in terminal state errors, successive pulses are applied until the desired position is reached. An unknown parameter that is a function of friction and inertia is adapted, which is subsequently used to calculate the pulse width. With the static and Coulomb friction model used in Ref. [2], the friction force is considered constant because the proposed technique guarantees unidirectional motion of the system. Rathbun [3] extended the pulse width control to a flexible two mass spring damper system. He used the single pulse to study the stability bounds on the pulse widths. Although the controller is stable, the flexible mode excited by the input pulse will result in undesirable residual vibration. If the damping is small, the settling time will increase, which will increase the maneuver time. Singh and Vadali [4,5] developed time-delay filtering techniques to preshape reference inputs, which result in the elimination of residual vibration of the flexible systems. This involves design of a prefilter that cancels the underdamped poles of the system. Robustness to variations in frequency and damping is achieved by placing additional zeros of the time-delay filter at the expected location of the complex poles of the system. This technique was further applied to systems with limited actuator bandwidth by imposing a constraint on the time rate of change of the control input [6]. However, the time-delay filtering technique can only be used for linear systems. Although the friction phenomena exhibits a hard nonlinearity near-zero velocity, the friction force will act as a bias input force to the linear system, if the velocity does not change signs during the maneuver. With this friction biased input, techniques for the design of control profiles for linear systems can be exploited. Kim and Singh [7] applied linear programming to find the control profiles of the system with the friction biased input force. The positive velocity constraints of the frictional body is imposed in addition to the boundary conditions and control input bounds in the design of the controller. The control profile resulting from the linear programming shows that stiction occurs during the maneuver for small command displacements. Therefore, friction force cannot be considered constant during stiction. In this paper, a three pulse control profile is first proposed with user-selected pulse width. The pole-zero cancellation technique in conjunction with an iterative method of solving this problem is presented. This is followed by studying the restriction on the control input to maintain positive velocity of the first mass. If stiction occurs during the maneuver, the control profile has to be modified, as illustrated in Sec. 7. Numerical simulations are performed to verify the proposed controllers.

2 Problem Formulation

The floating oscillator under the influence of friction is illustrated in Fig. 1, where m_1, m_2 are the first and second mass, k is the spring constant, u the control input, f the friction force, and x_1, x_2 are the positions of the first and second mass. The equation of motion of the system can be written as

$$M\ddot{\underline{x}} + K\underline{x} = D(u - f) \tag{1}$$

where M, K, D, and $\underline{x}$ are

$$M = \begin{bmatrix} m_1 & 0 \\ 0 & m_2 \end{bmatrix}, \quad K = \begin{bmatrix} k & -k \\ -k & k \end{bmatrix}, \quad D = \begin{bmatrix} 1 \\ 0 \end{bmatrix}, \quad \underline{x} = \begin{bmatrix} x_1 \\ x_2 \end{bmatrix} \tag{2}$$

The friction force is modeled as a static nonlinear function of the velocity that accounts for static and Coulomb friction. The friction model can be represented as:

$$f(\underline{x},u) = \begin{cases} f_c\, sgn(\dot{x}_1) & \text{if } \dot{x}_1 \neq 0 \\ f_s\, sgn(u_s) & \text{if } \dot{x}_1 = 0 \text{ and } u_s > f_s \\ u_s & \text{if } \dot{x}_1 = 0 \text{ and } u_s \leqslant f_s \end{cases} \tag{3}$$

where f_s is the static friction, f_c is the Coulomb friction, and u_s is the sum of the forces applied to the first mass, which is

$$u_s = u + k(x_2 - x_1). \tag{4}$$

If the velocity of the first mass never goes to zero and stays positive during the maneuver, the friction force for a rest-to-rest maneuver becomes

$$f = f_c[1 - H(t - T_f)] \tag{5}$$

where $H(\cdot)$ is the Heaviside step function and T_f is the final time. With this friction model, Eq. (1) becomes

Contributed by the Dynamic Systems, Measurements, and Control Division of The American Society of Mechanical Engineers. Manuscript received July 21, 2003. Final manuscript received September 15, 2004. Associate Editor: Santosh Devasia.

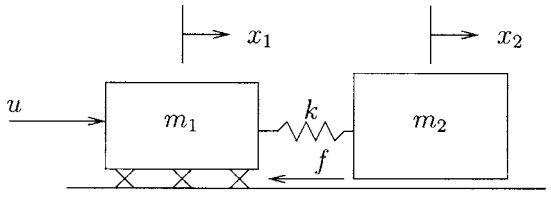

Fig. 1 Floating oscillator under friction

$$M\ddot{\underline{x}} + K\underline{x} = D\{u - f_c[1 - H(t - T_f)]\}. \tag{6}$$

It is more convenient to study the floating oscillator system if the decoupled equation of motion is used. Define new decoupled states $\underline{z}=[\theta, q]^T$, where θ and q denote the rigid and flexible body states of the system. The transformation matrix V can be formed from the eigenvectors of the system, which decouples the system with the relationship $\underline{x}=V\underline{z}$. The decoupled state equation is

$$\begin{bmatrix} \ddot{\theta} \\ \ddot{q} \end{bmatrix} + \begin{bmatrix} 0 & 0 \\ 0 & \omega^2 \end{bmatrix} \begin{bmatrix} \theta \\ q \end{bmatrix} = \begin{bmatrix} \dfrac{1}{m_1 + m_2} \\ -\dfrac{1}{m_1 + m_2} \end{bmatrix} \{u - f_c[1 - H(t - T_f)]\} \tag{7}$$

where V and ω are

$$V = \begin{bmatrix} 1 & -\dfrac{m_2}{m_1} \\ 1 & 1 \end{bmatrix}, \quad \omega = \sqrt{\frac{k(m_1 + m_2)}{m_1 m_2}} \tag{8}$$

For a rest-to-rest maneuver problem, the boundary conditions are

$$x_1(0) = x_2(0) = 0 \quad x_1(T_f) = x_2(T_f) = d$$

$$\dot{x}_1(0) = \dot{x}_2(0) = 0 \quad \dot{x}_1(T_f) = \dot{x}_2(T_f) = 0 \tag{9}$$

where d is the desired position at T_f and the corresponding boundary conditions of the decoupled states are

$$\theta(0) = \dot{\theta}(0) = 0 \quad \theta(T_f) = d, \quad \dot{\theta}(T_f) = 0$$

$$q(0) = \dot{q}(0) = 0 \quad q(T_f) = \dot{q}(T_f) = 0. \tag{10}$$

3 Pole-Zero Cancellation

In our development, a three pulse profile is initially assumed, as shown in Fig. 2(*a*). The control profile results in an active control period of time T_3, at which point the system is traveling with nonzero velocity. Following the implementation of the third pulse, the system is allowed to coast to rest. The pulse widths are selected by the user, which can correspond to the sampling time or an integral multiple of the sampling time of the digital implementation of the controller. The pulse amplitudes are subsequently determined to satisfy the boundary conditions. Since the velocity state of the first mass is assumed to remain positive over the duration of the maneuver, the new input to the linear system is biased by the magnitude of Coulomb friction, as shown in Fig. 2(*b*). The Coulomb friction biased input can be parametrized as

$$u(t) - f_c[1 - H(t - T_f)] = (A_0 - f_c) - A_1 H(t - T_1) + A_2 H(t - T_2) - A_3 H(t - T_3) + f_c H(t - T_f). \tag{11}$$

This biased input $u(t)-f_c[1-H(t-T_f)]$ can be generated by a time-delay filter with a transfer function

$$G(s) = (A_0 - f_c) - A_1 e^{-sT_1} + A_2 e^{-sT_2} - A_3 e^{-sT_3} + f_c e^{-sT_f} \tag{12}$$

when it is subject to a unit step input. Since the control input in Fig. 2(*a*) should be zero for $t \geqslant T_3$, we arrive at the constraint

$$A_0 - A_1 + A_2 - A_3 = 0. \tag{13}$$

In order to eliminate the vibration at the end of the maneuver, a pair of zeros of the transfer function [Eq. (12)], should cancel the flexible mode poles of the system [4]. To cancel the flexible mode poles, the real and imaginary parts of the transfer function $G(s)$ evaluated at $s=j\omega$, should be equated to zero resulting in the equations:

$$A_0 - A_1 \cos \omega T_1 + A_2 \cos \omega T_2 - A_3 \cos \omega T_3 = f_c(1 - \cos \omega T_f) \tag{14}$$

$$-A_1 \sin \omega T_1 + A_2 \sin \omega T_2 - A_3 \sin \omega T_3 = -f_c \sin \omega T_f \tag{15}$$

The displacement of the rigid body at the final time is the sum of the rigid body displacement at $t=T_3$ and the coasting displacement:

$$\theta(T_f) = \theta(T_3) + \frac{m_1 + m_2}{2f_c}[\dot{\theta}(T_3)]^2 = d. \tag{16}$$

$\theta(T_3)$ and $\dot{\theta}(T_3)$ are found by solving the rigid body differential equation:

$$\theta(T_3) = \frac{1}{2(m_1 + m_2)} \times [A_0(T_3)^2 - A_1(T_3 - T_1)^2 + A_2(T_3 - T_2)^2 - f_c(T_3)^2] \tag{17}$$

$$\dot{\theta}(T_3) = \frac{1}{m_1 + m_2}[A_0 T_3 - A_1(T_3 - T_1) + A_2(T_3 - T_2) - f_c T_3]. \tag{18}$$

The final time can be found by adding the coasting time to T_3. Since satisfying Eqs. (14) and (15) is equivalent to the flexible states being forced to zero at the final time, the coasting time is found by solving the rigid body equation for $t > T_3$ and by equating the velocity of the rigid body to be zero. The resulting final time is

$$T_f = T_3 + \frac{\dot{\theta}(T_3)(m_1 + m_2)}{f_c} = \frac{1}{f_c}(A_1 T_1 - A_2 T_2 + A_3 T_3) \tag{19}$$

The solution of the multipulse controller is determined by solving Eqs. (13)–(16) that results in four nonlinear equations in four unknowns $A_{0,1,2,3}$. An iterative approach for solving for the final time and the pulse amplitudes will be presented in the next section.

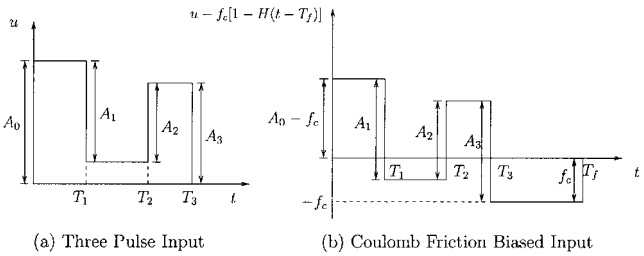

Fig. 2 Input profile

4 Iterative Solution Approach

If the flexible motion states $q(T_f)$ and $\dot{q}(T_f)$ are forced to zero at the final time, residual vibration will be eliminated. Since the final time in Eq. (19) is a function of pulse amplitudes, Eqs. (14) and (15) are difficult to solve. To address this problem, the states of the flexible mode at $t=T_3$ that will force the flexible motion to be zero at the final time are derived. Solutions of the flexible mode equation at $t=T_3$ are

$$q(T_3) = -\frac{1}{\omega^2(m_1+m_2)}[-f_c - A_0\cos\omega T_3 + A_1\cos\omega(T_3-T_1) - A_2\cos\omega(T_3-T_2) + A_3 + f_c\cos\omega T_3] \quad (20)$$

$$\dot{q}(T_3) = -\frac{1}{\omega(m_1+m_2)}[A_0\sin\omega T_3 - A_1\sin\omega(T_3-T_1) + A_2\sin\omega(T_3-T_2) - f_c\sin\omega T_3]. \quad (21)$$

The equation of motion of the flexible mode for the coasting period with initial conditions $q(T_3)$ and $\dot{q}(T_3)$ is

$$\ddot{q}_c + \omega^2 q_c = \frac{f_c[1-H(t-T_c)]}{m_1+m_2} \quad (22)$$

where q_c is the flexible mode state for the coasting period and the coasting time $T_c = T_f - T_3$. The solution to Eq. (22) is

$$q_c(t) = \frac{f_c}{m_1+m_2}\left[\left(\frac{1}{\omega^2} - \frac{\cos\omega t}{\omega^2}\right) - \left(\frac{1}{\omega^2} - \frac{\cos\omega(1-T_c)}{\omega^2}\right) \times H(t-T_c)\right] + q(T_3)\cos\omega t + \frac{\dot{q}(T_3)\sin\omega t}{\omega} \quad (23)$$

$$\dot{q}_c(t) = \frac{f_c}{m_1+m_2}\left(\frac{\sin\omega t}{\omega}\right) - q(3\Delta t)\omega\sin\omega t + \dot{q}(3\Delta t)\cos\omega t. \quad (24)$$

At $t = T_c$, the flexible motion should be eliminated. By substituting T_c into Eqs. (23) and (24) and equating them to zero, the flexible states at $t = T_3$ that will force the flexible states to zero at the final time are

$$\begin{bmatrix} q(T_3) \\ \dot{q}(T_3) \end{bmatrix} = \begin{bmatrix} -\dfrac{f_c(\cos\omega T_c - 1)}{\omega^2(m_1+m_2)} \\ -\dfrac{f_c\sin\omega T_c}{\omega(m_1+m_2)} \end{bmatrix}. \quad (25)$$

The flexible states at $t = T_3$ shown in Eq. (25) will force the flexible motion to be eliminated at the end of the maneuver if T_c is known. However, the total maneuver time is a function of pulse amplitudes and therefore, an iterative approach is used to find the total maneuver time and T_c. Rewriting the constraint, Eqs. (13), (20), and (21) in terms of A_1, A_2, and A_3, the constraint equations in matrix form become

$$\begin{bmatrix} -1 & 1 & -1 \\ -\cos\omega(T_3-T_1) & \cos\omega(T_3-T_2) & -1 \\ -\sin\omega(T_3-T_1) & \sin\omega(T_3-T_2) & 0 \end{bmatrix}\begin{bmatrix} A_1 \\ A_2 \\ A_3 \end{bmatrix} = \begin{bmatrix} -1 \\ -\cos\omega T_3 \\ -\sin\omega T_3 \end{bmatrix} A_0 + \begin{bmatrix} 0 \\ f_c\cos\omega T_3 - f_c + \omega^2(m_1+m_2)q(T_3) \\ f_c\sin\omega T_3 - \omega(m_1+m_2)\dot{q}(T_3) \end{bmatrix}. \quad (26)$$

To find initial values for the input pulse amplitudes and final time, solve Eq. (26) for A_1, A_2, and A_3 in terms of A_0 by letting $q(T_3) = \dot{q}(T_3) = 0$. By substituting A_1, A_2, and A_3 into the rigid body constraint in Eq. (16), A_0 can be determined. Once the pulse amplitudes are found, the final time is found by substituting the pulse amplitudes into Eq. (19). With this initial T_f, flexible states at $t = T_3$ are computed using Eq. (25). The new pulse amplitudes and total maneuver time is calculated with these new flexible states at $t = T_3$. This procedure is repeated until the flexible states and final time converge.

Instead of the iterative approach proposed in the paper an optimization problem can be posed to minimize T_c subject to the constraints given by Eqs. (16), (19), (25), and (26), where the variables to be solved for are A_0, A_1, A_2, A_3, and T_c. We have verified the solution generated by the iterative algorithm and it is coincident with that of the optimization algorithm.

5 Bounds on Control Pulse

The multiple pulse input development so far allows the user to select pulse widths for the prescribed displacement. However, bounds on pulse amplitudes should be examined because of the positive velocity constraint. The first pulse amplitude A_0 should be greater than the static friction, f_s. Also, the pulse amplitude should be less than the permitted peak input amplitude, u_p. Therefore, the bounds on A_0 become

$$f_s < A_0 \leqslant u_p \quad (27)$$

The velocity of the first mass can be written as

$$\dot{x}_1(t) = \frac{1}{m_1+m_2}[(A_0-f_c)g(t) - A_1 g(t-T_1)H(t-T_1) + A_2 g(t-T_2)H(t-T_2) - A_3 g(t-T_3)H(t-T_3)] \quad (28)$$

where $g(t)$ is a function defined by the following equation.

$$g(t) = t + \frac{m_2\sin\omega t}{m_1\omega} \quad (29)$$

For $0 < t < T_1$, Eq. (28) reduces to

$$\dot{x}_1(t) = \frac{A_0 - f_c}{m_1+m_2}g(t) \quad (0 < t < T_1) \quad (30)$$

Rathbun [3] showed that the selection of a specific mass ratio guarantees positive velocity of the first mass for $0 < t < T_1$. Since A_0 is greater than f_c, Eq. (30) is always positive if $g(t)$ is positive. Rewriting the equation for $g(t)$ yields

$$g(t) = t\left(1 + \frac{m_2}{m_1}\frac{\sin\omega t}{\omega t}\right) = t\left[1 + \frac{m_2}{m_1}\mathrm{sinc}(\omega t)\right] > 0 \quad (31)$$

Knowing that $-0.2172 < \mathrm{sinc}(\omega t) < 1$, Eq. (31) results in bounds on the ratio of the first and the second mass that guarantees positive velocity, which is

$$\frac{m_1}{m_2} > 0.2172. \quad (32)$$

For systems that violate this mass ratio, multipulse control profiles can also be designed. However, the model of the system will be represented by a series of piecewise linear systems that makes solving the problem significantly more difficult. The local maximum and minimum of $g(t)$ coincides with the time when the velocity of the first mass reaches its local maximum and minimum. The time derivative of $g(t)$ is

$$\dot{g}(t) = 1 + \frac{m_2}{m_1}\cos\omega t \quad (33)$$

It is patent that $\dot{g}(t)$ is always positive and hence $g(t)$ is a monotonically increasing function if

$$\frac{m_1}{m_2} \geqslant 1 \quad (34)$$

If $0.2172 < m_1/m_2 < 1$, $g(t)$ is always positive but not a monotonically increasing function. Similarly, the velocity of the first mass for $T_1 < t < T_2$ becomes

$$\dot{x}_1(t) = \frac{A_0 - f_c}{m_1+m_2}g(t) - \frac{A_1}{m_1+m_2}g(t-T_1) \quad (T_1 < t < T_2). \quad (35)$$

The first mass velocity will reach its minimum or maximum values for $T_1 < t < T_2$ when

$$\ddot{x}_1(t) = \frac{1}{m_1 + m_2} \times \left[A_0 - A_1 - f_c + \frac{(A_0 - f_c)m_2}{m_1} \cos \omega t - \frac{A_1 m_2}{m_1} \cos \omega (t - T_1) \right] = 0 \quad (36)$$

Solving Eq. (36) for t, the velocity of the first mass will have extreme values when

$$t_{\min,\max} = \frac{1}{\omega} \left[\sin^{-1}\left(-\frac{C}{D} \right) - \phi + 2n\pi \right] \quad (37)$$

where, C, D, and ϕ are defined as

$$C = A_0 - A_1 - f_c$$

$$D = \sqrt{\left[\frac{m_2(A_0 - f_c - A_1 \cos \omega T_1)}{m_1} \right]^2 + \left[\frac{-m_2 A_1 \sin \omega T_1}{m_1} \right]^2}$$

$$\phi = \tan^{-1}\left(-\frac{A_0 - f_c - A_1 \cos \omega T_1}{A_1 \sin \omega T_1} \right) \quad (38)$$

The solution $t_{\min,\max}$ might have none or multiple solutions for a different integer value of n because $t_{\min,\max}$ should lie in the interval $[T_1\ T_2]$. Therefore, the minimum velocity of the first mass in this interval becomes

$$\min(\dot{x}_1) = \begin{cases} \min[\dot{x}_1(T_1), \dot{x}_1(T_2), \dot{x}_1(t_{\min,\max})] & \text{if } 0.2172 < m_1/m_2 < 1 \\ \min[\dot{x}_1(T_1), \dot{x}_1(T_2)] & \text{if } m_1/m_2 > 1 \end{cases} \quad (39)$$

Therefore, the constraint on the pulse amplitudes for positive velocity for $T_1 < t < T_2$ can be derived from Eq. (35), which is

$$A_1 < (A_0 - f_c) \frac{g(t_{\min})}{g(t_{\min} - T_1)} \quad (40)$$

where $t_{\min}$ is the time when the velocity of the first mass is at its minimum. If this condition is violated, stiction of the first mass will occur. The control profile should be modified because the constant friction assumption is no longer valid. For $T_2 < t < T_3$, positive A_2 will guarantee positive velocity of the first mass, provided the velocity is positive for $t < T_2$. The velocity of the first mass for $T_3 < t < T_f$ is

$$\dot{x}_1(t) = \dot{\theta}(T_3) - \frac{f_c}{m_1 + m_2} \left[(t - T_3) + \frac{m_2 \sin \omega (t - T_f)}{m_1 \omega} \right] \quad (41)$$

According to Eq. (41), the velocity of the first mass never goes to zero if the mass ratio satisfies the condition shown in Eq. (32). Equation (41) is a monotonically decreasing function if $m_1/m_2 < 1$.

6 Numerical Simulation

Numerical simulations are used to illustrate the performance of the proposed controllers. The parameter values used in the simulation are shown in Table 1. The first simulation is performed with the initial and final states of

$$x_1(0) = x_2(0) = 0 \quad x_1(T_f) = x_2(T_f) = 0.1$$

$$\dot{x}_1(0) = \dot{x}_2(0) = 0 \quad \dot{x}_1(T_f) = \dot{x}_2(T_f) = 0. \quad (42)$$

The pulse widths are chosen such that $T_1 = 0.1$ s, $T_2 = 0.2$ s, and $T_3 = 0.3$ s. If the condition number of the matrix on the left-hand side of Eq. (26) is large, or if the resulting solution is one that violates Eq. (27), one has to select a different pulse width. The controller for this problem is shown in Fig. 3 and the corresponding response of the system is plotted in Fig. 4. The solid line and the dashed line represent the states of the first and second masses, respectively. It is shown that the first mass velocity is always positive and therefore unidirectional friction force is applied to the system during the maneuver. The system begins to coast at $t = 0.3$ s and the undesirable vibration is eliminated at the final time. The response plot of the decoupled states are also shown in Fig. 5. The flexible state at $t = 0.3$ is forced such that at the final time the flexible states become zero.

Figure 6 illustrates the variation of the pulse input amplitude change as a function of commanded displacement. The pulse widths are selected to be $T_1 = 0.04$ s, $T_2 = 0.08$ s, and $T_3 = 0.12$ s. For this specific pulse width, the velocity of the mass goes to zero

Table 1 Parameters used in the simulation

Symbol	Description	Value
m_1	Mass 1	80 Kg
m_2	Mass 2	100 Kg
ω	Natural frequency	50 rad/s
u_p	Peak input	1000 N
f_s	Static friction	137 N
f_c	Coulomb friction	111 N

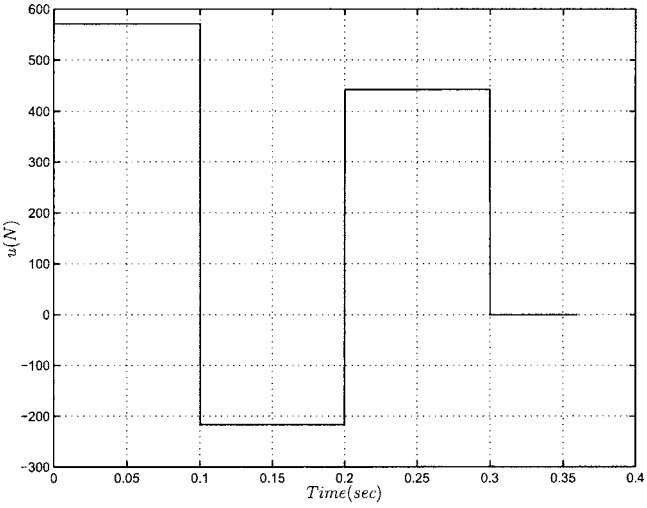

Fig. 3 Three pulse control input (d=0.1)

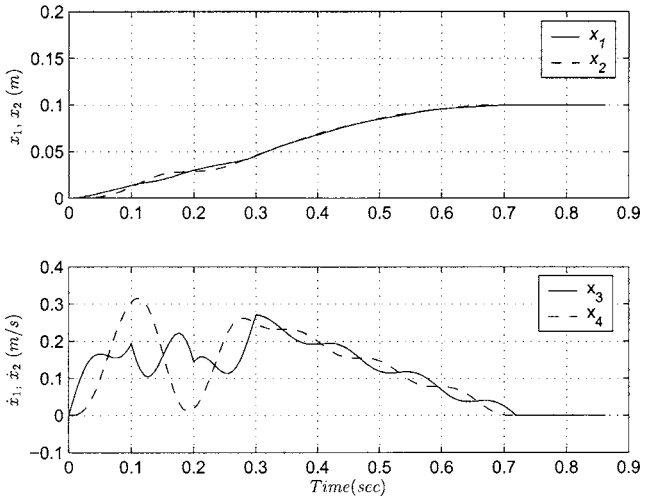

Fig. 4 Response of the system (d=0.1 m)

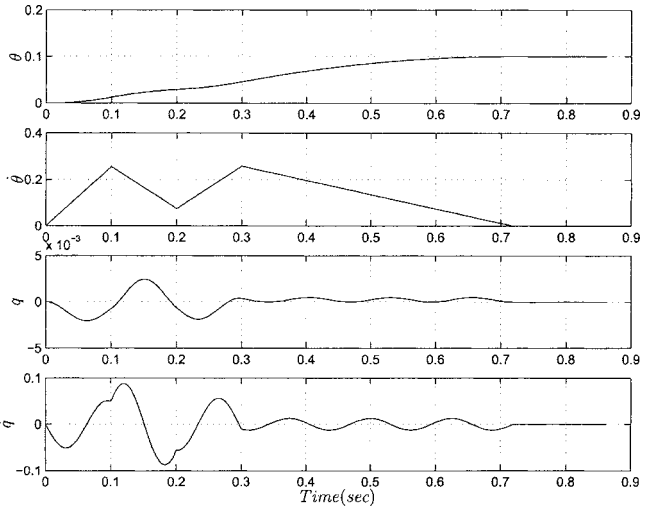

Fig. 5 Response of the system, decoupled states (d=0.1 m)

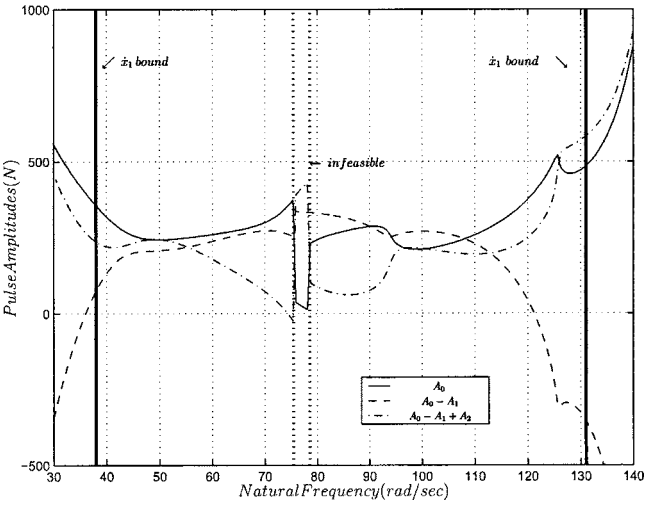

Fig. 7 Pulse amplitudes versus natural frequency

during the maneuver for d=0.0039 m, which corresponds to the lower displacement bound with the chosen pulse widths. For a displacement of d=0.278 m, the control input saturates, which corresponds to the upper displacement bound for the prescribed pulse width. The upper and lower bounds can be changed by selecting pulses of different width.

The relationship of the pulse input amplitudes for different natural frequency values is illustrated in Fig. 7. It is also shown in Fig. 7 that there are no feasible solutions that exist in the frequency range from 76 to 79 rad/s. This is because the matrix in Eq. (26) becomes singular when the switching time is chosen, such that:

$$\omega(T_3 - T_2) = 2n\pi \quad \text{or} \quad \omega(T_3 - T_1) = 2n\pi \tag{43}$$

where n is a positive integer. Therefore different pulse widths should be selected for designing a controller if the pulse widths chosen make the condition number of the matrix in Eq. (26) very large.

Incorrect estimates of the friction and frequency of the system result in a steady-state error and residual vibration at the final time. Figure 8 represents the steady-state error of the first mass with respect to variations in the spring constant and Coulomb friction. It can be seen that the final displacement is more sensitive to the friction variation compared to variations in the frequency. Robustness to the frequency variation can be obtained with additional pulses, which corresponds to the freedom to place additional zeros of the time-delay filter at the estimated flexible pole locations. The friction variation can be handled by a successive application of the proposed control profile until the desired position is reached. Stability of the iterative operation is guaranteed for bounded friction and spring constant variations if the steady-state error remains less than 100%. The performance of the controller can be enhanced if the uncertain/varying parameters are adapted during the iterative application of the input. Figure 9 shows the variation of the residual energy with respect to the variations in friction and spring constant. The total residual energy includes the energy from the residual vibration of the second mass, in addition to the norm of the steady-state error of the first mass. It can be seen that if the friction coefficient is overestimated, the residual energy increases at a rate greater than when the friction coefficient is underestimated.

7 Systems With Stiction

When the command displacement is small, it may not be feasible to find a solution that will guarantee positive velocity of the first mass. If the velocity becomes zero during the maneuver, stiction might occur. If stiction is considered in the controller design, the control profile is assumed to be, as shown in Fig. 10. In the figure, τ is the time when the velocity of the first mass becomes

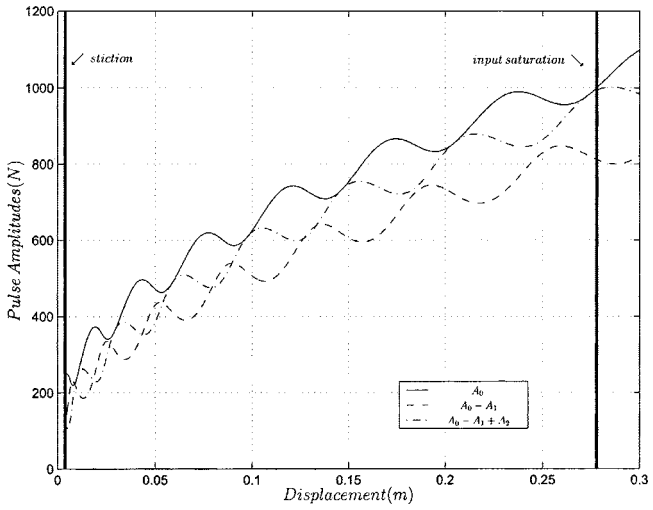

Fig. 6 Pulse amplitudes versus displacement

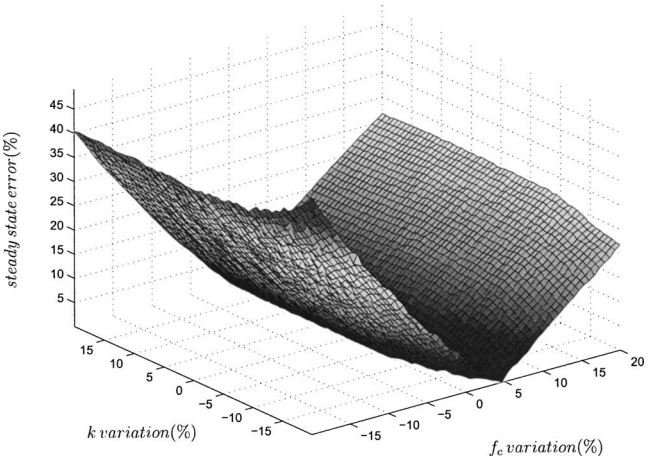

Fig. 8 Steady-state error with friction and spring constant variation

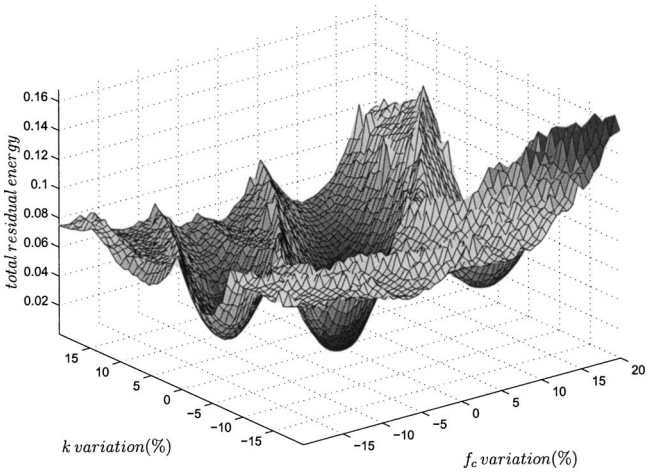

Fig. 9 Total residual energy with friction and spring constant variation

zero and the controller assumes that the first mass stays stuck for $\tau \leqslant t \leqslant T_3$. During stiction, the sum of the applied forces to the first mass should be less than or equal to the static friction value. Since the input is zero during the stiction, the condition of staying stuck becomes

$$|k[x_2(t) - x_1(t)] \leqslant f_s| \quad (\tau \leqslant t \leqslant T_3) \tag{44}$$

If the above condition is not met, the spring force has to be compensated to force the first mass to stay stuck for $\tau \leqslant t \leqslant T_3$. Spring force compensation is considered later in the section. Define the relative displacement and velocity at $t = T_3$ as

$$\eta_0 = x_2(T_3) - x_1(T_3), \quad \dot{\eta}_0 = \dot{x}_2(T_3) \tag{45}$$

First, η_0, $\dot{\eta}_0$, and A_3 are determined that will satisfy the boundary condition without the residual vibration at the final time. The flexible states at $t = T_4$ in terms of η_0 and $\dot{\eta}_0$ are

$$q(T_4) = -\frac{1}{\omega^2(m_1 + m_2)} \times [A_3 - f_c - A_3 \cos \omega(T_4 - T_3) + f_c \cos \omega(T_4 - T_3)] + \frac{m_1 \cos \omega(T_4 - T_3)}{m_1 + m_2}\eta_0 + \frac{m_1 \sin \omega(T_4 - T_3)}{\omega(m_1 + m_2)}\dot{\eta}_0 \tag{46}$$

$$\dot{q}(T_4) = -\frac{1}{\omega(m_1 + m_2)}[A_3 \sin \omega(T_4 - T_3) - f_c \sin \omega(T_4 - T_3)] - \frac{m_1 \omega \sin \omega(T_4 - T_3)}{m_1 + m_2}\eta_0 + \frac{m_1 \cos \omega(T_4 - T_3)}{m_1 + m_2}\dot{\eta}_0 \tag{47}$$

Equations (46) and (47) are solved for η_0 and $\dot{\eta}_0$.

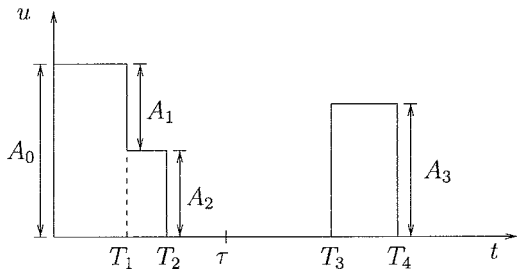

Fig. 10 Input profile with stiction

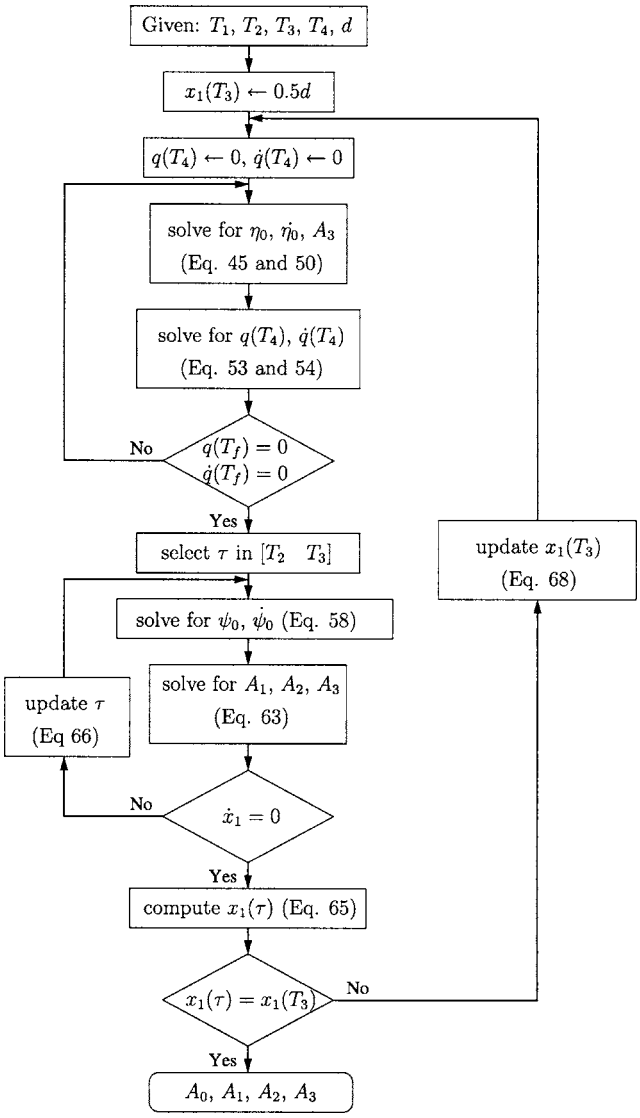

Fig. 11 Algorithm for the controller design under stiction

$$\begin{bmatrix} \eta_0 \\ \dot{\eta}_0 \end{bmatrix} = \begin{bmatrix} \dfrac{\cos \omega(T_4 - T_3) - 1}{m_1\omega^2} \\ \dfrac{\sin \omega(T_4 - T_3)}{m_1 \omega} \end{bmatrix} A_3 + \begin{bmatrix} \dfrac{f_c[1 - \cos \omega(T_4 - T_3)]}{m_1\omega^2} \\ -\dfrac{f_c \sin \omega(T_4 - T_3)}{m_1 \omega} \end{bmatrix} + \frac{m_1 + m_2}{m_1} \begin{bmatrix} \cos \omega(T_4 - T_3) & -\dfrac{\sin \omega(T_4 - T_3)}{\omega} \\ \omega \sin \omega(T_4 - T_3) & \cos \omega(T_4 - T_3) \end{bmatrix} \begin{bmatrix} q(T_4) \\ \dot{q}(T_4) \end{bmatrix} \tag{48}$$

The displacement boundary condition is

$$\theta(T_f) = \theta(T_4) + \frac{m_1 + m_2}{2f_c}[\dot{\theta}(T_4)]^2 = d \tag{49}$$

where $\theta(T_4)$ and $\theta(\dot{T}_4)$ are

$$\theta(T_4) = x_{1s} + \frac{A_3 - f_c}{2(m_1 + m_2)}(T_4 - T_3)^2 + \frac{m_2}{m_1 + m_2}[\eta_0 + \dot{\eta}_0(T_4 - T_3)] \tag{50}$$

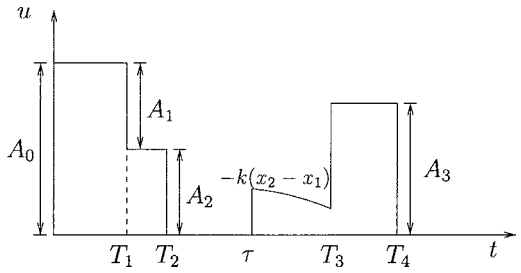

Fig. 12 Input profile with spring force compensation

$$\dot{\theta}(T_4) = \frac{A_3 - f_c}{m_1 + m_2}(T_4 - T_3) + \frac{m_2}{m_1 + m_2}\dot{\eta}_0 \tag{51}$$

x_{1s} is the first mass position under stiction, which is unknown. Therefore, an iterative procedure is required, starting with the initial x_{1s}. For small displacements, an initial x_{1s} close to half of the displacement to be moved serves as a good starting point. Then, η_0, $\dot{\eta}_0$, and A_3 can be computed similar to the approach for the nonstiction case. Assuming $q(T_4)=\dot{q}(T_4)=0$ initially, solve η_0 and $\dot{\eta}_0$ in terms of A_3 from Eq. (48). A_3 is found from the displacement boundary condition in Eq. (49). With the initial solutions of η_0, $\dot{\eta}_0$, and A_3, the flexible body states at $t=T_4$ that will eliminate the residual vibration are found as follows.

$$q(T_4) = -\frac{f_c(\cos \omega T_c - 1)}{\omega^2(m_1 + m_2)} \tag{52}$$

$$\dot{q}(T_4) = -\frac{f_c \sin \omega T_c}{\omega(m_1 + m_2)} \tag{53}$$

where the coasting time T_c is

$$T_c = \frac{1}{f_c}[(A_3 - f_c)(T_4 - T_3) + m_2 \dot{\eta}_0] \tag{54}$$

This procedure is repeated until the flexible states at $t=T_4$ and total maneuver time converge. Once η_0 and $\dot{\eta}_0$ are determined, the state constraints at $t=\tau$ should be found to solve for A_0, A_1, and A_2. However, τ is a function of the input pulse amplitudes that are not yet determined. Therefore an iterative approach is applied again with the initial assumption of τ. Because the stiction occurs between τ and T_3, the system behaves like a single mass harmonic oscillator such that

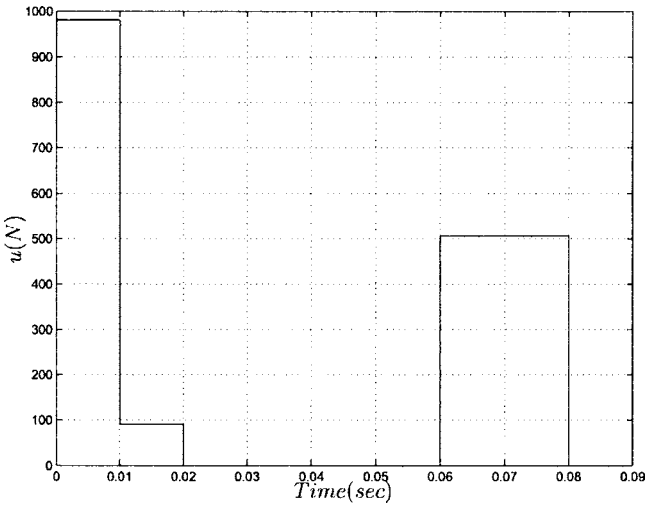

Fig. 13 Control input (d=0.01 m)

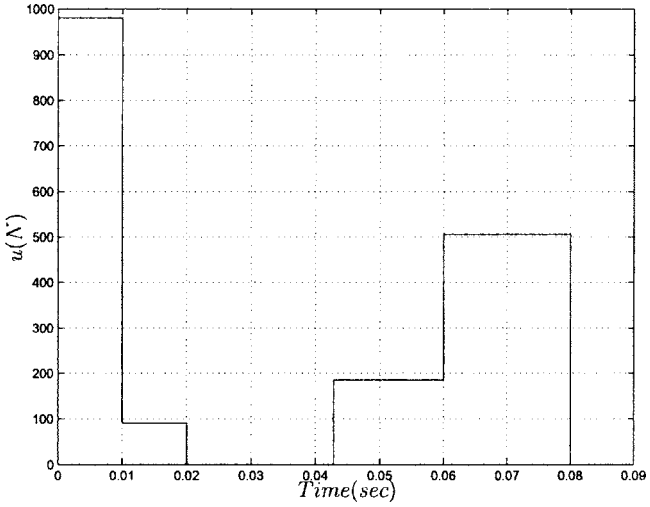

Fig. 14 Control input with spring force compensation (d = 0.01 m)

$$m_2\ddot{\psi} + k\psi = 0 \tag{55}$$

with the initial and final conditions

$$\psi_0 = x_2(\tau) - x_1(\tau) \quad \psi_f = x_2(T_3) - x_1(T_3) = \eta_0$$

$$\dot{\psi}_0 = \dot{x}_2(\tau) \quad \dot{\psi}_f = \dot{x}_2(T_3) = \dot{\eta}_0 \tag{56}$$

Since final states are specified, solving Eq. (55) for ψ_0 and $\dot{\psi}_0$ yields

$$\begin{bmatrix} \psi_0 \\ \dot{\psi}_0 \end{bmatrix} = \begin{bmatrix} \cos \omega_s(T_3 - \tau) & -\dfrac{\sin \omega_s(T_3 - \tau)}{\omega_s} \\ \omega_s \sin \omega_s(T_3 - \tau) & \cos \omega_s(T_3 - \tau) \end{bmatrix} \begin{bmatrix} \eta_0 \\ \dot{\eta}_0 \end{bmatrix} \tag{57}$$

where $\omega_s = \sqrt{k/m_2}$. Then the flexible states at $t=\tau$ are found in terms of ψ_0 and $\dot{\psi}_0$.

$$q(\tau) = \frac{m_1}{m_1 + m_2}\psi_0$$

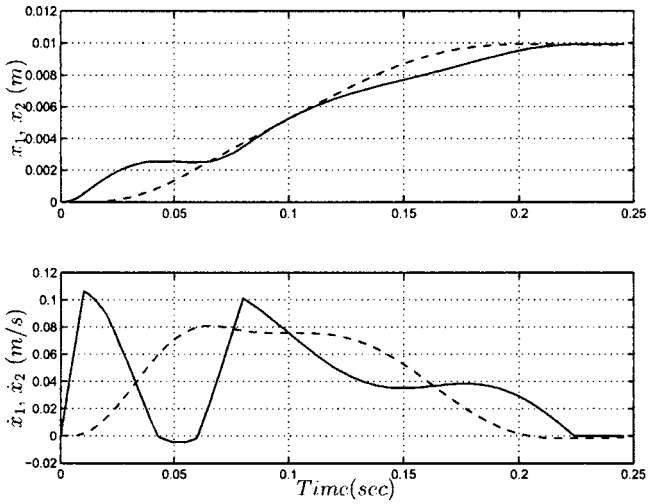

Fig. 15 System response without spring force compensation (d=0.01 m)

$$\dot{q}(\tau) = \frac{m_1}{m_1 + m_2}\dot{\psi}_0 \tag{58}$$

Constraint equations required to solve for A_0, A_1, and A_2 are

$$A_0 - A_1 - A_2 = 0 \tag{59}$$

$$q(\tau) = \frac{1}{\omega^2(m_1 + m_2)}[A_0 \cos \omega\tau - A_1 \cos \omega(\tau - T_1) - A_2 \cos \omega(\tau - T_2) + f_c(1 - \cos \omega\tau)] \tag{60}$$

$$\dot{q}(\tau) = -\frac{1}{\omega(m_1 + m_2)}[A_0 \sin \omega\tau - A_1 \sin \omega(\tau - T_1) - A_2 \sin \omega(\tau - T_2) - f_c \sin \omega\tau] \tag{61}$$

Because $q(\tau)$ and $\dot{q}(\tau)$ should satisfy Eq. (58), we have the following simultaneous equation.

$$\begin{bmatrix} 1 & -1 & -1 \\ \cos \omega\tau & -\cos \omega(\tau - T_1) & -\cos \omega(\tau - T_2) \\ \sin \omega\tau & -\sin \omega(\tau - T_1) & -\sin \omega(\tau - T_2) \end{bmatrix} \begin{bmatrix} A_0 \\ A_1 \\ A_2 \end{bmatrix} = \begin{bmatrix} 0 \\ m_1\omega^2\psi_0 - f_c(1 - \cos \omega\tau) \\ -m_1\omega\dot{\psi}_0 + f_c \sin \omega\tau \end{bmatrix} \tag{62}$$

The resulting A_0, A_1, and A_2 should satisfy the condition that the velocity of the first mass at $t = \tau$ becomes zero. The velocity of the first mass at $t = \tau$ can be written as:

$$\dot{x}_1(\tau) = \dot{\theta}(\tau) - \frac{m_2}{m_1}\dot{q}(\tau) = 0 \tag{63}$$

where $\dot{q}(\tau)$ is found from Eq. (58) and $\theta(\tau)$ is found from the following equation.

$$\theta(\tau) = \frac{1}{2(m_1 + m_2)}[A_0\tau^2 - A_1(\tau - T_1)^2 - A_2(\tau - T_2)^2 - f_c\tau^2] \tag{64}$$

If the velocity constraint of the first mass at $t = \tau$ is violated, the τ should be updated. Using the Newton-Raphson method, the new τ is updated by the following relationship.

$$\tau_{\text{new}} = \tau_{\text{old}} - \frac{\dot{x}_1(\tau_{\text{old}})}{\ddot{x}_1(\tau_{\text{old}})} \tag{65}$$

The procedure is repeated until τ satisfies the condition $\dot{x}_1(\tau) = 0$. The stuck position of the first mass with the converged τ becomes

$$x_1(\tau) = \theta(\tau) - \frac{m_2}{m1 + m2}\psi_0 \tag{66}$$

This value should agree with the value of x_{1s} chosen to determine η_0, $\dot{\eta}_0$, and A_3 shown in Eq. (50). If $x_1(\tau)$ results in a value larger than x_{1s}, the larger value of x_{1s} should be selected. Therefore, the new x_{1s} can be updated by the following relationship.

$$x_{1s,\text{new}} = x_{1s,\text{old}} + K[x_1(\tau) - x_{1s,\text{old}}] \tag{67}$$

where K is the update gain. The procedure of designing a controller discussed so far is summarized in Fig. 11.

The controller design so far assumes that the first mass stays stuck for $\tau \leqslant t \leqslant T_3$. However, if the spring force is large enough to move the first mass, the spring force should be compensated for the first mass to stay stuck. Therefore, the control input should be modified such that

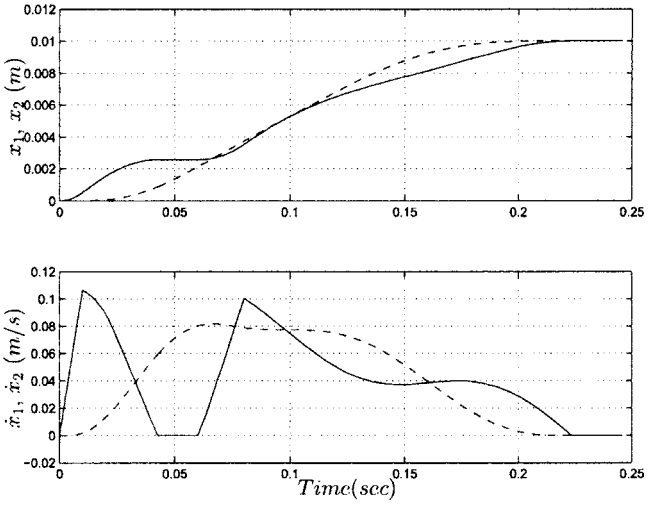

Fig. 16 System response with spring force compensation (*d* = 0.01 m)

$$u = -k\left[\psi_0 \cos \omega_s(t - \tau) - \dot{\psi}_0 \frac{\sin \omega_s(t - \tau)}{\omega_s}\right] \quad \tau < t < T_3 \tag{68}$$

The corresponding new control profile is shown in Fig. 12. It is also possible to compensate the spring force with a constant input force. Define $u_{\max}$ and $u_{\min}$ as the maximum and minimum input force for $\tau \leqslant t \leqslant T_3$. The constant input can be used for spring force compensation such that:

$$u = u_{\max} \quad \text{if } u_{\max} - u_{\min} < f_s(\tau \leqslant t \leqslant T_3) \tag{69}$$

8 Numerical Simulation for Systems Under Stiction

The boundary conditions to illustrate the design of the controller described in Sec. 7 are:

$$x_1(0) = x_2(0) = 0 \quad x_1(T_f) = x_2(T_f) = 0.01$$
$$\dot{x}_1(0) = \dot{x}_2(0) = 0 \quad \dot{x}_1(T_f) = \dot{x}_2(T_f) = 0 \tag{70}$$

The control profile parametrized to accommodate stiction is shown in Fig. 13. The pulse widths are selected such that $T_1 = 0.01$ s, $T_2 = 0.02$ s, $T_3 = 0.06$ s, and $T_4 = 0.08$ s. The corresponding state responses plotted in Fig. 15 show that the velocity of the first mass becomes negative because of the spring force acting on the first mass. Since the design process assumed that the first mass has zero velocity in the interval $\tau \leqslant t \leqslant T_3$, small residual vibration will exist at the final time. The velocity reversal can be prevented by compensating the spring force as shown in Fig. 14 and the corresponding response plot is shown in Fig. 16. The total maneuver time for this controller is smaller than the three pulse controller design (see Fig. 15–17).

The boundary conditions for the next example are

$$x_1(0) = x_2(0) = 0 \quad x_1(T_f) = x_2(T_f) = 0.001$$
$$\dot{x}_1(0) = \dot{x}_2(0) = 0 \quad \dot{x}_1(T_f) = \dot{x}_2(T_f) = 0 \tag{71}$$

The pulse widths are selected such that $T_1 = 0.005$ s, $T_2 = 0.01$ s, $T_3 = 0.09$ s, and $T_4 = 0.1$ s. With this controller, the responses of the system are plotted in Fig. 18. It is shown from the response plot that the first mass stops at a position that is very close to the halfway point of the desired final position. The first mass stays stuck without a compensation of the spring force because the spring force is smaller that the static friction value.

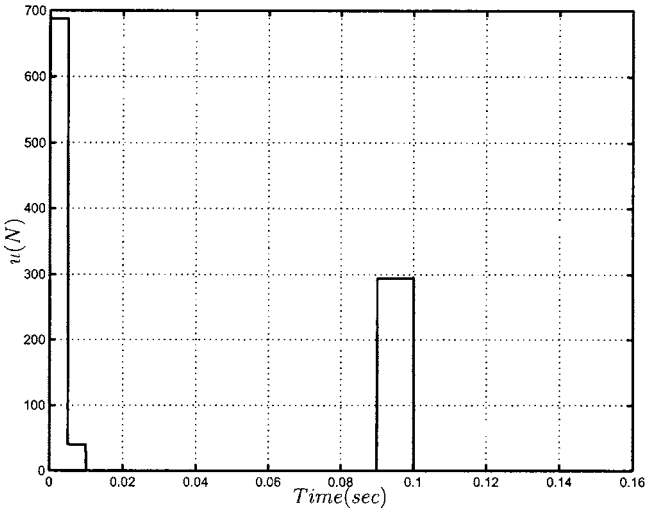

Fig. 17 Control input (d=0.001 m)

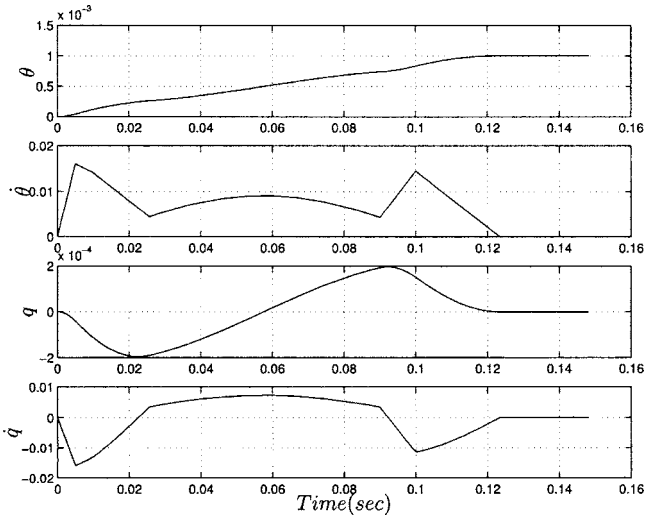

Fig. 19 Response of the system, decoupled states (d = 0.001 m)

9 Conclusions

In this work, design techniques for pulse amplitude modulated controllers are presented. A three pulse controller with user selected pulse width initiates the motion of the maneuvering system toward its final position and then exploits the friction force to bring the coasting system to rest. This assumes a unidirectional frictional force which requires that the mass which is subject to friction has a velocity profile that does not change sign. Variations in the pulse amplitude as a function of displacement and modal frequency is studied and it is noted that for specific frequencies, the proposed technique results in infeasible solutions. This problem can be addressed by selecting different pulse widths. Next, a modification of the three pulse control profile is proposed that can account for stiction and velocity reversals. This technique requires the spring force to be compensated if it is greater than the static friction. The proposed technique is illustrated in a frictional benchmark problem.

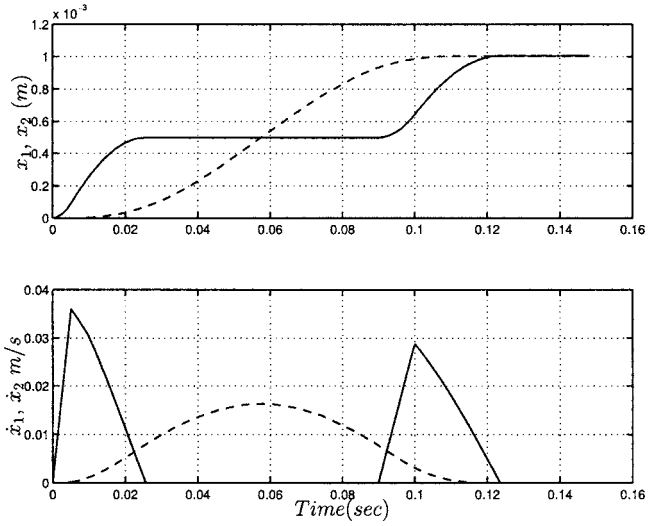

Fig. 18 Response of the system (d=0.001 m)

References

[1] Helouvry, B. A., Dupont, P., and De Wit, C. C., 1994, "A Survey of Models, Analysis Tools and Compensation Methods for the Control of Machines With Friction," Automatica, **30**, pp. 1083–1138.

[2] Sangsik, Y., and Tomizuka, M., 1998, "Adaptive Pulse Width Control for Precise Positioning Under the Influence of Static and Coulomb Friction," J. Dyn. Syst., Meas., Control, **110**, pp. 221–227.

[3] Rathbun, D. B., 2001, "Pulse Modulation Control for Flexible Systems Under the Influence of Nonlinear Friction," Ph.D dissertation, University at Washington.

[4] Singh, T., and Vadali, S. R., 1994, "Robust Time-Optimal Control: A Frequency Domain Approach," J. Guid. Control Dyn., **17**, pp. 346–353.

[5] Singh, T., and Vadali, S. R., 1995, "Robust Time-Delay Control of Multimode Systems," Int. J. Control, **62**, pp. 1319–1339.

[6] Muenchhof, M., and Singh, T., 2003, "Jerk Limited Time Optimal Control of Flexible Structures," J. Dyn. Syst., Meas., Control, **125**, pp. 139–142.

[7] Kim, J.-J., and Singh, Tarunraj, 2003, "Controller Design for Flexible Systems With Friction: Linear Programming Approach," *Proceedings of the American Control Conference*, pp. 4555–4560.